



## Enhancing the Photocatalytic Activity of Nickel Ferrite Doped with Graphene†

Bo XIAO<sup>1</sup> and SHOU-QING LIU<sup>1,2,\*</sup>

<sup>1</sup>Jiangsu Key Laboratory of Environmental Functional Materials; College of Chemistry and Bioengineering, Suzhou University of Science and Technology, Suzhou 215009, P.R. China

<sup>2</sup>Key Laboratory of Green Chemistry of Sichuan Institutes of Higher Education, Zigong 643000, P.R. China

\*Corresponding author: Tel/Fax: +86 512 69209055; E-mail: shouqing\_liu@hotmail.com

Published online: 1 March 2014;

AJC-14780

Graphene-nickel ferrite (G-NiFe<sub>2</sub>O<sub>4</sub>) has been successfully synthesized using graphene, NiSO<sub>4</sub>·6H<sub>2</sub>O and FeCl<sub>3</sub>·6H<sub>2</sub>O as the raw materials by the hydrothermal method at 180 °C for 10 h. The as-synthesized sample was characterized by X-ray diffraction, Fourier transform infrared spectroscopy, scanning electron microscopy, transmission electron microscopy and vibrating sample magnetometer at room temperature. The photo-Fenton degradations of methylene blue, rhodamine B and malachite green were conducted in the presence of oxalic acid using G-NiFe<sub>2</sub>O<sub>4</sub> as the photo-Fenton catalyst under visible light irradiation. The results showed that the G-NiFe<sub>2</sub>O<sub>4</sub> catalyst can effectively decompose the organic pollutants under visible light irradiation and the decolorization ratio of methylene blue in the concentration of 20 mg/L reached over 87.8 % in 10 h, whereas the decolorization ratio was only 28.8 % when the NiFe<sub>2</sub>O<sub>4</sub> was utilized as the catalyst under the similar conditions. The decolorization ratio maintained over 70 % after 8 runs *via* a magnetic field for separation, showing the G-NiFe<sub>2</sub>O<sub>4</sub> catalyst is stable and easily separable for utilization.

**Keywords:** Graphene, Nickel ferrite, Doping, Fenton catalyst, Photocatalysis.

### INTRODUCTION

Magnetically recoverable catalysts are very attractive due to their ease of separation from the reaction mixture system. Nickel ferrite, a magnetic material, can be used as a heterogeneous photo-Fenton catalyst for the degradation of organic pollutants under ultraviolet irradiation<sup>1</sup>. Unfortunately, ultraviolet light only makes up a 3 % proportion of solar light whereas visible light accounts for a 43 % proportion of solar irradiation. Therefore, extending the response of the material to solar light is desirable. Recent researches have shown that carbon materials are able to enhance the photocatalytic activities of catalysts. For example, the fullerene C<sub>60</sub> increases the photocatalytic activities of WO<sub>3</sub> and TiO<sub>2</sub><sup>2</sup>. A second example is that activated carbon improves the activity of TiO<sub>2</sub> catalyst<sup>3</sup>. Graphene (G), a carbon material, is also found to increase the activity of semiconductor photocatalysts<sup>4-6</sup>. However, doping nickel ferrite with graphene for photocatalytic application has not been reported up to date. We combined nickel ferrite with graphene to fabricate the graphene-doping nickel ferrite (G-NiFe<sub>2</sub>O<sub>4</sub>) as a heterogeneous photo-Fenton catalyst for the degradation of organic pollutants under visible irradiation.

### EXPERIMENTAL

**Synthesis of G-NiFe<sub>2</sub>O<sub>4</sub>:** Graphene was synthesized using a modified Hummers and Offeman method<sup>7</sup>. G (0.234 g, 10 % of NiFe<sub>2</sub>O<sub>4</sub> mass used) was dispersed in 10 mL of deionized water. Then, NiSO<sub>4</sub>·6H<sub>2</sub>O (2.6285 g, 0.01 mol) and FeCl<sub>3</sub>·6H<sub>2</sub>O (5.4058 g, 0.02 mol) were separately dissolved in 15 mL of water. The solutions were mixed under stirring. NaOH (3.2000 g, 0.08 mol) was dissolved in 10 mL of deionized water, after which the solution was added dropwise to the mixed suspension solution under continuous stirring. Deionized water was also added to the suspension solution up to the final total volume of 60 mL. The suspension solution was then transferred into a 100 mL Teflon-lined stainless-steel autoclave that was sealed and maintained at 180 °C for 10 h. The suspension was filtered to obtain G-NiFe<sub>2</sub>O<sub>4</sub> precipitates, which were rinsed thrice with water to remove excess NaOH and other electrolytes. Finally, a magnetic powder was obtained after sintering at 200 °C for 4 h. The magnetic powder was used for characterization and photocatalytic tests. Pure NiFe<sub>2</sub>O<sub>4</sub> was prepared for comparison.

**Characterization for structure and magnetism:** X-Ray diffraction (XRD) measurements were performed using an

†Presented at The 7th International Conference on Multi-functional Materials and Applications, held on 22-24 November 2013, Anhui University of Science & Technology, Huainan, Anhui Province, P.R. China

X'Pert-Pro MPD X-ray diffractometer (Panalytical, Netherland). The X-ray source was  $\text{CuK}\alpha$  radiation with a wavelength of 0.154 nm, tube voltage of 40 kV and tube current of 40 mA. A Fourier-transform infrared (FT-IR) spectrophotometer (Spectrum BX, PerkinElmer Ltd., USA) was used for the characterization of group vibrations at an optical resolution of  $4\text{ cm}^{-1}$ . The mulls of  $\text{G-NiFe}_2\text{O}_4$  were supported by a KBr plate. Magnetic measurements were made using a vibrating sample magnetometer (Lake Shore 7410, Lake Shore Cryotronics, Inc. USA) at  $25 \pm 2\text{ }^\circ\text{C}$ .

## RESULTS AND DISCUSSION

**XRD Characterization:** Fig. 1 presents the XRD pattern of the as-synthesized  $\text{NiFe}_2\text{O}_4$ ,  $\text{G-NiFe}_2\text{O}_4$  and graphene samples. The positions of the characteristic diffraction peaks ( $2\theta$ ) agree well with the data in the JCPDS card (No. 74-2081) of  $\text{NiFe}_2\text{O}_4$ , verifying the same crystal structure of the as-synthesized  $\text{G-NiFe}_2\text{O}_4$  as that of  $\text{NiFe}_2\text{O}_4$ .

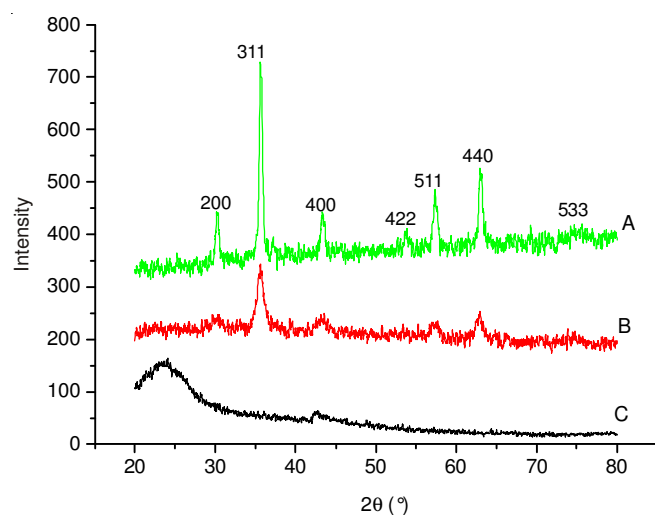


Fig. 1. XRD patterns of the samples. A,  $\text{NiFe}_2\text{O}_4$ ; B,  $\text{G-NiFe}_2\text{O}_4$ ; C, G

The broadened peaks of the  $\text{G-NiFe}_2\text{O}_4$  and  $\text{NiFe}_2\text{O}_4$  samples indicate that the  $\text{NiFe}_2\text{O}_4$  and  $\text{G-NiFe}_2\text{O}_4$  particles are very small<sup>8</sup>. The average diameters ( $D$ ) of the as-synthesized  $\text{NiFe}_2\text{O}_4$  and  $\text{G-NiFe}_2\text{O}_4$  particles were calculated to be 9.4 and 10.3 nm using the Debye-Scherrer equation  $D = K\lambda/(W \cos \theta)$  at a diffraction angle of  $35.59^\circ$  ( $2\theta$ ), respectively.  $W$  is the breadth of the observed diffraction peak at its half height,  $K$  is the so-called shape factor (usually 0.9) and  $\lambda$  is the wavelength of the X-ray source used (0.154 nm by our measurement).

**FT-IR characterization:** Fig. 2 shows an absorption band located at  $598\text{ cm}^{-1}$ , which is assigned to tetrahedral metal stretching vibrations. Another band is observed at  $412\text{ cm}^{-1}$ , corresponding to octahedral metal stretching vibrations<sup>9</sup>. The absorption band at  $3414\text{ cm}^{-1}$  is assigned to adsorbed water hydroxyl ions and that at  $2366\text{ cm}^{-1}$  is assigned to carbon dioxide<sup>9</sup>. The band at  $1628\text{ cm}^{-1}$  is attributed to  $\text{C}=\text{C}$  stretching vibrations as part of the ring breathing mode in the graphene skeleton. The asymmetric and symmetric stretching vibrations of  $\text{C-H}$  bonds at  $2935$  and  $2850\text{ cm}^{-1}$  and bands at  $1032$ ,  $1117\text{ cm}^{-1}$  show the graphene has been doped in nickel ferrite<sup>10</sup>.

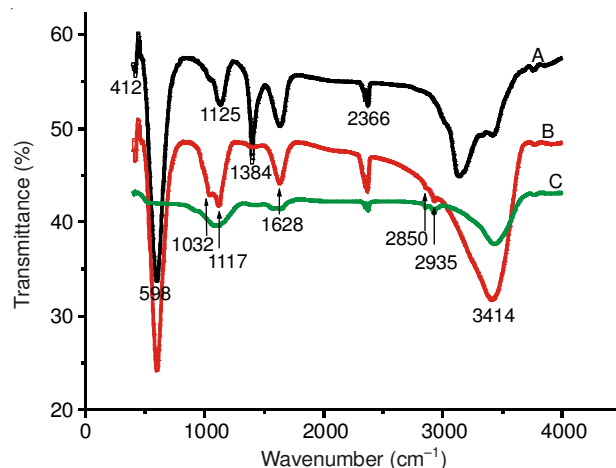


Fig. 2. FT-IR spectra of the samples. (A),  $\text{NiFe}_2\text{O}_4$ ; (B),  $\text{G-NiFe}_2\text{O}_4$ ; (C), G

**Magnetic characterization:** Magnetization hysteresis loops of the as-synthesized  $\text{G-NiFe}_2\text{O}_4$  and  $\text{NiFe}_2\text{O}_4$  samples at room temperature were measured using a vibrating sample magnetometer (Fig. 3). The saturation magnetization of  $\text{NiFe}_2\text{O}_4$  was  $40.4\text{ emu/g}$ , whereas that of  $\text{G-NiFe}_2\text{O}_4$  was  $75.3\text{ emu/g}$ . The value for  $\text{G-NiFe}_2\text{O}_4$  is larger than that for  $\text{NiFe}_2\text{O}_4$ , showing that  $\text{G-NiFe}_2\text{O}_4$  is more separable than  $\text{NiFe}_2\text{O}_4$ .

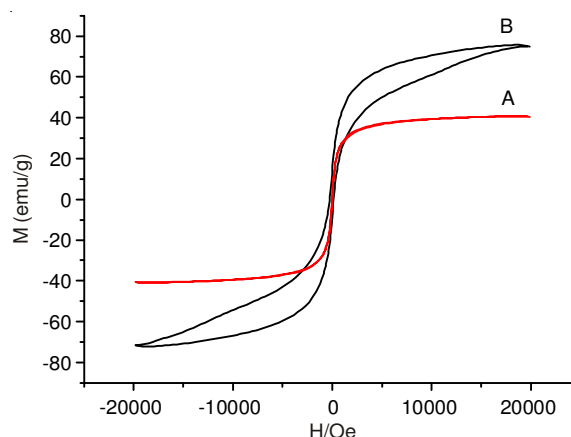


Fig. 3. Magnetization curves of  $\text{NiFe}_2\text{O}_4$  (A) and  $\text{G-NiFe}_2\text{O}_4$  (B) samples

**Photocatalytic degradation of organic pollutants:** Fig. 4 displays the degradation curves of methylene blue using  $\text{G-NiFe}_2\text{O}_4$  as catalyst in the presence or absence of oxalic acid under visible light irradiation or non-irradiation. Curve A shows a  $87.8\%$  decolorization ratio for methylene blue using  $\text{G-NiFe}_2\text{O}_4$  as the Fenton-like catalyst in the presence of  $1.0\text{ mM H}_2\text{C}_2\text{O}_4$  under visible light irradiation for 10 h, whereas the decolorization ratio is only  $28.8\%$  (curve B) when pure  $\text{NiFe}_2\text{O}_4$  was used as the catalyst under similar conditions, indicating that  $\text{G-NiFe}_2\text{O}_4$  responds to visible light. In the case of absence of the  $\text{G-NiFe}_2\text{O}_4$  catalyst, the decolorization ratio is very low (curve C), showing the significance of the  $\text{G-NiFe}_2\text{O}_4$  species used as a catalyst during the photo-catalytic degradation process of the decolorization reactions. Curve D shows the oxalic acid is vital to the decolorization during the photocatalytic process. Curve E shows little adsorption for methylene blue.

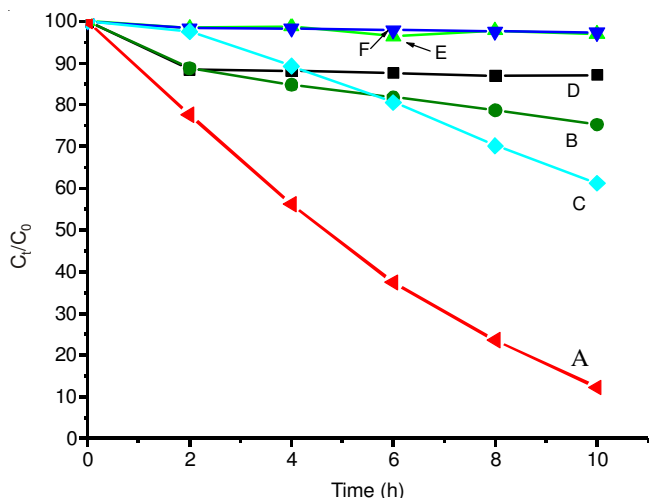


Fig. 4. Degradation curves of methylene blue. The initial conditions  $C(\text{methylene blue}) = 20 \text{ mg/L}$ ,  $m(\text{G-NiFe}_2\text{O}_4) = 0.1 \text{ g}$ ,  $C(\text{H}_2\text{C}_2\text{O}_4) = 1.0 \text{ mmol/L}$ , the total volume = 50.0 mL. (A), G-NiFe<sub>2</sub>O<sub>4</sub> + H<sub>2</sub>C<sub>2</sub>O<sub>4</sub> + methylene blue under visible light irradiation; (B), NiFe<sub>2</sub>O<sub>4</sub> + H<sub>2</sub>C<sub>2</sub>O<sub>4</sub> + methylene blue under visible light irradiation; (C), H<sub>2</sub>C<sub>2</sub>O<sub>4</sub> + methylene blue under visible light irradiation; (D), G-NiFe<sub>2</sub>O<sub>4</sub> + H<sub>2</sub>C<sub>2</sub>O<sub>4</sub> + methylene blue in dark; (E), G-NiFe<sub>2</sub>O<sub>4</sub> + methylene blue under visible light irradiation; (F), G-NiFe<sub>2</sub>O<sub>4</sub> + methylene blue in dark

Subsequent researches showed that the G-NiFe<sub>2</sub>O<sub>4</sub> catalyst enables to speed degrading rhodamine B and malachite green in the presence of oxalic acid under visible light irradiation as shown in Fig. 5, showing the generalization property of the catalyst during photocatalytic degradation of organic pollutants.

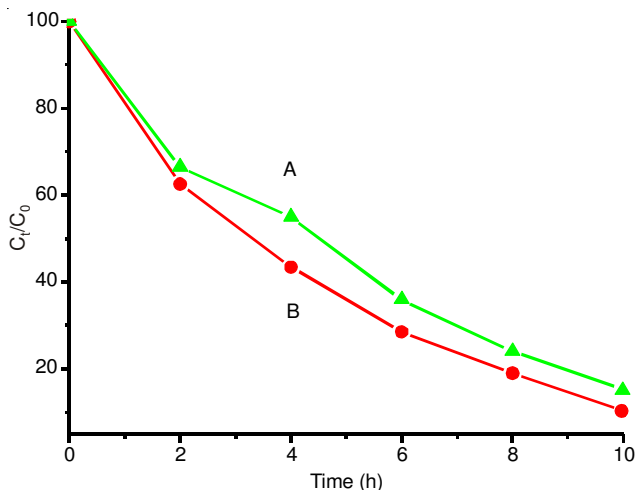


Fig. 5. Degradation curves of rhodamine B and malachite green. The initial conditions:  $C(\text{H}_2\text{C}_2\text{O}_4) = 1.0 \text{ mmol/L}$ ,  $m(\text{G-NiFe}_2\text{O}_4) = 0.1 \text{ g}$ ,  $C(\text{methylene blue}) = 20 \text{ mg/L}$ ,  $C(\text{rhodamine-B}) = 20 \text{ mg/L}$ ,  $C(\text{MG}) = 20 \text{ mg/L}$ , the total volume = 50 mL. A: H<sub>2</sub>C<sub>2</sub>O<sub>4</sub> + G-NiFe<sub>2</sub>O<sub>4</sub> + RhB under visible light irradiation; B: H<sub>2</sub>C<sub>2</sub>O<sub>4</sub> + G-NiFe<sub>2</sub>O<sub>4</sub> + MG under visible light irradiation

## Conclusion

The as-synthesized G-NiFe<sub>2</sub>O<sub>4</sub> species enables to speed the degradation of organic pollutants in the presence of both oxalic acid under visible light irradiation whereas NiFe<sub>2</sub>O<sub>4</sub> species fails under similar conditions. Thus, graphene plays a vital role of photocatalytic process in absorption of visible light.

## ACKNOWLEDGEMENTS

This work is financially supported by the National Natural Science Foundation of China (No.21347006), Education Department of Jiangsu Province (No. 12KJA430005), Ministry of Housing and Urban-Rural Development of China (No. 06-K4-26), the Opening Project of Key Laboratory of Green Chemistry of Sichuan Institutes of Higher Education (No. LZJ1304) and the Project Funded by the Priority Academic Program Development of Jiangsu Higher Education Institutions, China.

## REFERENCES

1. S.Q. Liu, L.R. Feng, N. Xu, Z.G. Chen and X.M. Wang, *Chem. Eng. J.*, **203**, 432 (2012).
2. Z.-D. Meng, L. Zhu, J.-G. Choi, M.-L. Chen and W.-C. Oh, *J. Mater. Chem.*, **21**, 7596 (2011).
3. X.W. Zhang, M.H. Zhou and L.C. Lei, *Carbon*, **43**, 1700 (2005).
4. Z. Peining, A.S. Nair, P. Shengjie, Y. Shengyuan and S. Ramakrishna, *ACS Appl. Mater. Interfaces*, **4**, 581 (2012).
5. M.S.A. Sher Shah, A.R. Park, K. Zhang, J.H. Park and P.J. Yoo, *ACS Appl. Mater. Interfaces*, **4**, 3893 (2012).
6. C. Liu, Y. Teng, R. Liu, S. Luo, Y. Tang, L. Chen and Q. Cai, *Carbon*, **49**, 5312 (2011).
7. W. Hummers Jr. and R. Offeman, *J. Am. Chem. Soc.*, **80**, 1339 (1958).
8. S.K. Kurinec, N. Okeke, S.K. Gupta, H. Zhang and T.D. Xiao, *J. Mater. Sci.*, **41**, 8181 (2006).
9. M. Mouallem-Bahout, S. Bertrand and O. Pena, *J. Solid State Chem.*, **178**, 1080 (2005).
10. M. Acik, C. Mattevi, C. Gong, G. Lee, K. Cho, M. Chhowalla and Y.J. Chabal, *ACS Nano*, **4**, 5861 (2010).